

See discussions, stats, and author profiles for this publication at: <https://www.researchgate.net/publication/221742295>

Differences between Protein Dynamics of Hemoglobin upon Dissociation of Oxygen and Carbon Monoxide

ARTICLE *in* JOURNAL OF THE AMERICAN CHEMICAL SOCIETY · JANUARY 2012

Impact Factor: 12.11 · DOI: 10.1021/ja209659w · Source: PubMed

CITATIONS

4

READS

21

3 AUTHORS, INCLUDING:



Masako Nagai

Hosei University

69 PUBLICATIONS 862 CITATIONS

SEE PROFILE

Differences between Protein Dynamics of Hemoglobin upon Dissociation of Oxygen and Carbon Monoxide

Yuka Murakawa,[†] Masako Nagai,^{‡,§} and Yasuhisa Mizutani^{*,⊥}

[†]Graduate School of Science and Technology, Kobe University, Nada, Kobe 657-8501, Japan

[‡]Research Center for Micro-Nano Technology, Hosei University, Tokyo 184-0003, Japan

[§]Department of Frontier Bioscience, Faculty of Engineering, Hosei University, Tokyo 184-8584, Japan

[⊥]Department of Chemistry, Graduate School of Science, Osaka University, 1-1 Machikaneyama, Toyonaka 560-0043, Japan

S Supporting Information

ABSTRACT: Protein dynamics of human adult hemoglobin (HbA) upon ligand photolysis of oxygen (O₂) and carbon monoxide (CO) was investigated using time-resolved resonance Raman (TR³) spectroscopy. The TR³ spectra of the both photoproducts at 1-ns delay differed from that of the equilibrium deligated form (deoxy form) in the frequencies of the iron–histidine stretching [$\nu(\text{Fe-His})$] and methine wagging (γ_7) modes, and the band intensity of pyrrole stretching and substituent bending (ν_8) modes. Spectral changes of the O₂ photoproduct in the submicrosecond region were faster than those of the CO photoproduct, indicating that the structural dynamics following the photodissociation is ligand dependent for HbA. In contrast, no ligand dependence of the dynamics was observed for myoglobin, which has a structure similar to that of the subunit of HbA. The structural dynamics and relevance to the functionality of HbA also are discussed.

Protein dynamics plays a pivotal role in understanding protein function. In numerous biological processes, protein structural changes accompanying a reaction at a specific site must undergo global structural changes to perform a biological function, known as allostery.¹ The molecular mechanism of cooperativity in oxygen binding of hemoglobin (Hb) is a classical problem in this aspect. Human adult hemoglobin A (HbA) has an $\alpha_2\beta_2$ tetramer structure, exhibiting positive cooperativity in oxygen binding. X-ray crystallographic studies have demonstrated the presence of two distinct quaternary structures that correspond to the low-affinity (T or tense) and high-affinity (R or relaxed) states. The complete unligated (deoxy) structure typically assumes the T state, while the ligated form assumes the R state.² The cooperative oxygen binding of HbA has been explained in terms of a reversible transition between the two quaternary states upon partial ligation of four hemes.^{3,4} The large amplitude motions at the quaternary level, which form a communication link at the subunit interface, are driven by changes in the tertiary structure upon ligation. In this respect, myoglobin (Mb), which is structurally very similar to a subunit of HbA, serves as a model system for the tertiary relaxation processes.

In HbA, the heme is an iron–protoporphyrin IX, in which the Fe²⁺ ion is bound to the proximal histidine (His) as the

only covalent link to the protein. The heme iron binds diatomic molecules, such as O₂, CO, and NO, at the opposite side of the proximal His. The binding of small ligands to the hemes in HbA is a highly localized perturbation. However, this localized perturbation initiates a sequence of propagating structural events that culminates in a change of quaternary structure, proceeding from the T state to the R state. X-ray crystallography has provided extensive information about the end-point equilibrium structures.^{5,6} However, the mechanism by which deligation triggers structural rearrangements remains unclear. The most promising method for elucidating this mechanism is observation of the dynamics from one equilibrium species to the other in a site-specific manner.

Time-resolved resonance Raman (TR³) spectroscopy provided information about the dynamics of the tertiary and quaternary structures of heme proteins. Along with the studies of Gibson,⁷ numerous kinetic studies of hemeproteins by ligand photolysis techniques have been reported.^{8–12} However, TR³ studies on HbA were conducted mainly for dynamic investigations about CO photolysis. Very few studies on structural dynamics upon O₂ photolysis have been reported,^{13,14} even though the physiological ligand of HbA is O₂. Time-resolved measurements following O₂ photolysis are rarely reported for several reasons. First, the quantum yield of O₂ photolysis is low in hemeproteins. Second, in the presence of O₂, the heme iron is gradually autoxidized. Thus, a fraction of the sample becomes inactive for ligand binding during the measurements, making it difficult to accumulate data over long periods to improve the signal-to-noise ratio with a limited amount of the protein sample. Third, CO is usually assumed to be a good analogue for O₂. However, the validity of this assumption has been not been examined. The study of protein dynamics related to O₂ dissociation is essential to understanding the allostery of HbA because O₂ is its physiological ligand. This communication describes the TR³ spectra of HbA upon O₂ dissociation. Striking differences were found between the protein dynamics of HbA upon O₂ and CO dissociation and the evidence that CO is not a good analogue for O₂ in HbA. The characteristics of the primary protein response of HbA are discussed based on comparison of the results of HbA with those of Mb.

Received: October 18, 2011

Published: January 10, 2012



Figure 1 shows TR³ spectra for HbA upon O₂ and CO dissociation. Contribution of the ligated HbA was subtracted in

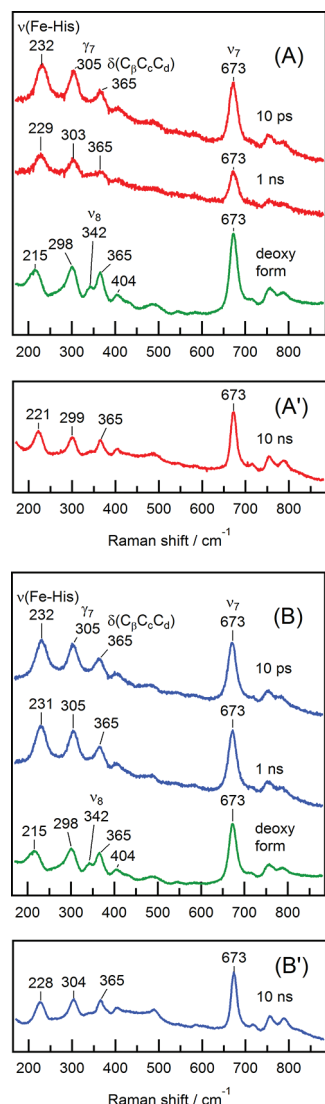


Figure 1. Picosecond time-resolved resonance Raman spectra of HbA upon O₂ dissociation [(A) and (A')] and CO dissociation [(B) and (B')].

the spectra. The subtraction parameter was determined so that ν_4 band characteristic to the ligated HbA completely disappeared in the difference spectra (Figure S1 in Supporting Information). The bands at 232, 305, 365, and 673 cm⁻¹ in the spectrum for 10-ps delay in panel A are assigned to vibrations of the heme. For O₂ dissociation, band intensities at 1 ns were weakened due to geminate recombination (GR) of O₂ in nanoseconds, while that of CO occurs in tens of nanoseconds. The large peak at 232 cm⁻¹ arises from the stretching mode of the covalent bond between the heme iron and N_ε of proximal His, $\nu(\text{Fe-His})$.¹⁵ The peak at 305 cm⁻¹ is an out-of-plane mode (γ_7 ; methine wagging).¹⁶ The peak at 365 cm⁻¹ is a substituent mode, $\delta(\text{C}_\beta\text{C}_\alpha\text{C}_\alpha)$, involving deformation of the propionate methylene groups.¹⁶ The peak at 673 cm⁻¹ is an in-plane mode (ν_7 , breathing-like mode of the porphyrin inner ring). The differences between the spectra of dissociated species and the deoxy form were observed in several bands both for O₂ and CO dissociation. First, the band at 342 cm⁻¹ (ν_8

band) in the deoxy form is weak or absent in the dissociated species. Second, the positions of γ_7 and $\nu(\text{Fe-His})$ bands of the dissociated species differ from those of the deoxy form. These results suggest the heme structure is not fully relaxed within a nanosecond for HbA, and are consistent with the results of nanosecond¹³ and picosecond¹⁷ TR³ experiments for CO dissociation.

Some distinct differences between CO- and O₂-dissociated species are shown in Figure 1. For CO dissociation, the frequency of the $\nu(\text{Fe-His})$ and γ_7 bands did not change substantially at 10 ns. In contrast, the $\nu(\text{Fe-His})$ and γ_7 bands downshifted in the 10-ns spectrum for O₂ dissociation. Scott and Friedman reported resonance Raman spectra of transient species measured with single intense nanosecond pulse (~10 ns) at high temperature.¹³ The reported spectra of the CO- and O₂-dissociated species are similar to each other, contrary to the present results. The difference between the present results and theirs would be mainly due to differences between sample temperatures and methods of the measurements: using single nanosecond pulse, spectra of photoproduct averaged within 10-ns duration were observed in their measurements.

Together with the TR³ data of HbA in the nanosecond region (Figure S2 in Supporting Information), the positions of the $\nu(\text{Fe-His})$ and γ_7 bands of HbA were analyzed, and plotted against delay time (Figure 2). Panels A and B show the position

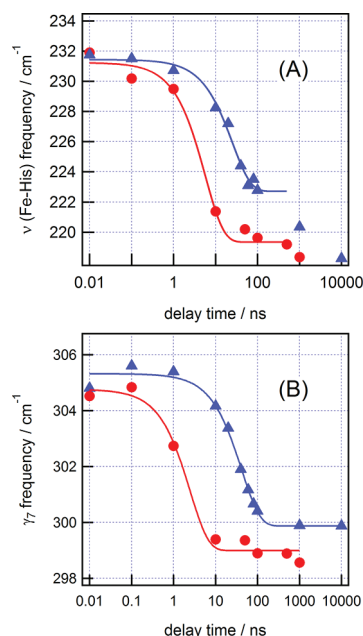


Figure 2. Temporal changes in (A) $\nu(\text{Fe-His})$ and (B) γ_7 frequencies of HbA following ligand photolysis. Circles and triangles represent data for O₂ and CO dissociation, respectively. The temporal shift of the $\nu(\text{Fe-His})$ band was fitted using a single exponential function, yielding time constants of 5.7 ± 1.3 and 25.4 ± 3.5 ns for O₂ and CO dissociation, respectively. The temporal shift of the γ_7 band was fitted using a single exponential function, yielding time constants of 2.5 ± 0.6 and 43.5 ± 3.8 ns, for O₂ and CO dissociation, respectively. For $\nu(\text{Fe-His})$ frequency, data up to 100 ns were fitted because a change in a microsecond phase overlapped the region later than 1 μ s.

of the $\nu(\text{Fe-His})$ and γ_7 bands, respectively. In both panels, red circles and blue triangles represent the data for O₂ and CO dissociation, respectively. Spectral changes occurred about one order of magnitude faster for O₂ dissociation than for CO

dissociation. These data demonstrate that the structural dynamics of HbA following ligand dissociation is ligand dependent.

Figure 3 shows TR³ spectra for Mb upon O₂ and CO dissociation. For Mb, the spectrum at 10-ps delay closely

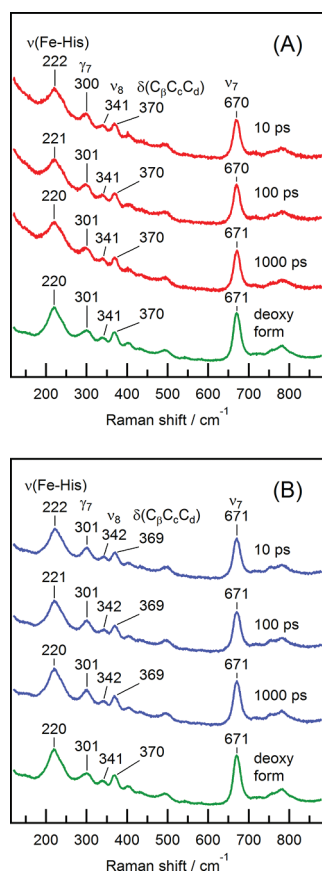


Figure 3. Picosecond time-resolved resonance Raman spectra of Mb upon (A) O₂ and (B) CO dissociation. Spectra of deoxy Mb are depicted at the bottom for comparison.

resembles the deoxy spectrum for both CO and O₂ dissociation except for a small frequency shift of the $\nu(\text{Fe-His})$ band, which was reported previously.¹⁸ No ligand dependence was observed in the TR³ spectra of Mb. These data contrast those related to HbA.

For HbA, ligand-dependent spectral changes were observed, including a frequency shift of the γ_7 and $\nu(\text{Fe-His})$ bands. The HbA adopts a metastable structure within a few picoseconds and does not significantly change in the subnanosecond to nanosecond time after CO dissociation.¹⁷ The metastable structure was characterized by higher frequencies of the γ_7 and $\nu(\text{Fe-His})$ modes compared to those of the deoxy form. This intermediate undergoes structural changes in the submicrosecond time frame. In contrast, the present study showed that the resonance Raman spectra of Mb for the dissociated species were similar for the O₂ and CO dissociation. A previous study on Mb revealed that the structure of the heme changes to one closely resembling the deoxy form within a few picoseconds.¹⁸ These experimental data indicate that structural dynamics to the heme later than a nanosecond are specific to HbA and are ligand dependent, suggesting that these changes are associated with allostery of HbA.

Previous time-resolved absorption¹⁹ and resonance Raman^{17,20,21} spectroscopic studies on HbA have established a series of intermediates following CO dissociation. In primary intermediate B, the heme structure changes to a metastable form similar to that of the deoxy form, but no detectable difference was found in globin structure between intermediate B and the CO-bound form. Protein relaxation leads to the secondary intermediate, R_{deoxy}. In the transition from B to R_{deoxy}, the distal E helix displaces toward the heme plane, probably driven by motion of the proximal F helix in response to Fe-His bond relaxation.^{20–22} For CO photolysis, this displacement occurs in tens of nanoseconds, which is the same order of magnitude as for the $\nu(\text{Fe-His})$ and γ_7 bands changes. The structural change seen beyond 10 ps for the heme in HbA does not indicate an intrinsic change in the nature of the heme group but is associated with structural changes of the globin (protein moiety), because the spectral changes of the heme were completed within a few picoseconds for a model compound without the protein matrix.¹⁸ Therefore, we can speculate that the structural changes of the heme are associated with the EF helical motion and that this motion is ligand dependent in HbA. A striking difference in interaction of the heme-bound ligand and the E helix was found between the oxy and carbonmonoxy forms of HbA. In the oxy form, the bound O₂ is hydrogen-bonded to the distal histidine, which is in the E helix. In contrast, no such interaction in the CO-bound form exists between the bound CO and the E helix. A difference in the interaction would cause a change in the structure of the EF helical section. This explains the ligand dependence of the protein dynamics of HbA.

Another possible explanation for the ligand-dependent spectral evolution of the dissociated species is that the spectra evolve due to change of depletion of homogeneous subensembles within the conformationally heterogeneous ensemble, which is known as kinetic hole burning.^{23,24} Figure

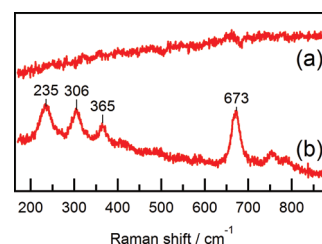


Figure 4. Difference spectra with reference to the spectrum of the O₂-dissociated species at 10 ps. (a) difference between the CO- and O₂-dissociated species at 10 ps. (b) difference between the O₂-dissociated species at 1 ns and 10 ps.

4 shows difference spectra with reference to the spectrum of the O₂-dissociated species at 10 ps. Trace a shows a difference spectrum between the CO- and O₂-dissociated species at 10 ps. The Raman intensity of both dissociated species has been normalized using the band intensity of the ν_7 mode. Trace b is a difference spectrum between the spectra of the O₂-dissociated species at 1 ns and 10 ps. The $\nu(\text{Fe-His})$ and γ_7 bands located at higher frequency than those of the O₂-dissociated species at 1 ns. The higher proximal strain in HbA is, the lower the frequencies of the $\nu(\text{Fe-His})$ and γ_7 bands are. Assuming that the probability of photodissociation is independent of conformational substates for O₂- and CO-bound forms of HbA, then the initial photoproduct population which

represents a random distribution of photoproduct conformations should be the same. This is indeed observed at 10 ps as shown in Figure 4a. There is a major difference in the subsequent evolution; whereas for the CO-dissociated species there is no subnanosecond GR, there is significant GR for the O₂-dissociated species. If there is a distribution of functionally distinct tertiary conformational substates that undergo GR for the oxy sample, then the Raman spectrum of the dissociated species will reflect the spectrum of the slowly recombining remaining population that has not undergone GR under the condition that interconversion between the fast- and slowly recombining substates is efficiently slow. The slowly recombining remaining population should have $\nu(\text{Fe-His})$ and γ_7 bands that show evidence of being more like the quasi stable ligand-dissociated R species rather than the unrelaxed ligand-dissociated R state population. This interpretation is consistent with the spectrum of the O₂-dissociated species at 1 ns in Figure 1. Similarly, the depleted component in the TR³ spectra for the O₂-dissociated species corresponds to the substate which had undergone GR if the interconversion between the fast- and slowly recombining substates is efficiently slow. Figure 4b shows a spectrum of the component at 1 ns. The observed features of the $\nu(\text{Fe-His})$ and γ_7 bands are consistent with the hypothesis of kinetic hole burning described above.

Kinetic hole burning has been observed at cryogenic temperatures and higher temperatures.^{23–25} It has been observed for band III in the near IR region (~760 nm). This band shift was found to be correlated with the $\nu(\text{Fe-His})$ frequency.²⁶ The difference between CO and O₂ with respect to kinetic hole burning was predicted based on the low population of GR for O₂ photoproduct at liquid helium temperatures.²⁷ These support the idea that the highest affinity conformations for Hb have lowest proximal strain, which results in highest $\nu(\text{Fe-His})$ frequency and reddest band III wavelengths, and undergo this subnanosecond and subpicosecond GR that gives rise to the high geminate yield.²⁶ The present data can be interpreted with the idea that the spectra evolve due to the change of depletion of homogeneous subensembles within the conformationally heterogeneous ensemble.

The present data indicates that the O₂- and CO-dissociated species show the differences in structural relaxation and/or in the distribution of conformational substates. Namely, the ensemble-averaged structural evolution of the O₂-dissociated species is not same with that of the CO-dissociated species. The structural dynamics of HbA, particularly for faster time scales, has been studied mainly for CO photolysis because of the difficulties in performing O₂ photolysis experiments. Even though CO is not a physiological ligand, the studies using CO photolysis have contributed to the understanding of allostery of HbA. However, the present results demonstrate that the models obtained from CO photolysis experiments should be reexamined using time-resolved studies on O₂ photolysis to understand the cooperative O₂ binding of HbA.

■ ASSOCIATED CONTENT

● Supporting Information

Experimental procedures, data analysis and nanosecond TR³ spectra of HbA upon ligand photolysis. This material is available free of charge via the Internet at <http://pubs.acs.org>.

■ AUTHOR INFORMATION

Corresponding Author

mztn@chem.sci.osaka-u.ac.jp

■ ACKNOWLEDGMENTS

This work was supported in part by a Grant-in-Aid for Scientific Research (B) (Grant No. 17350009) to Y.M. from the Japan Society for the Promotion of Science and by a Grant-in-Aid for Scientific Research on the Priority Area "Molecular Science for Supra Functional Systems" (Grant No. 19056013) to Y.M. from the Ministry of Education, Science, Sports, and Culture of Japan.

■ REFERENCES

- (1) Monod, J.; Wyman, J.; Changeux, J.-P. *J. Mol. Biol.* **1965**, *12*, 88.
- (2) Perutz, M. F. *Nature* **1970**, *228*, 726.
- (3) Perutz, M. F. *Annu. Rev. Biochem.* **1979**, *48*, 327.
- (4) Perutz, M. F.; Fermi, G.; Luisi, B.; Shaanan, B.; Liddington, R. C. *Acc. Chem. Res.* **1987**, *20*, 309.
- (5) Fermi, G.; Perutz, M. F.; Shaanan, B.; Fourme, R. *J. Mol. Biol.* **1984**, *175*, 159.
- (6) Baldwin, J. M. *J. Mol. Biol.* **1980**, *136*, 103.
- (7) Gibson, Q. H. *Biochem. J.* **1959**, *71*, 293.
- (8) Shank, C.; Ippen, E.; Bersohn, R. *Science* **1976**, *193*, 50.
- (9) Mizutani, Y.; Kitagawa, T. *Science* **1997**, *278*, 443.
- (10) Friedman, J. M. *Science* **1985**, *228*, 1273.
- (11) Greene, B. I.; Hochstrasser, R. M.; Weisman, R. B.; Eaton, W. A. *Proc. Natl. Acad. Sci. U.S.A.* **1978**, *75*, 5255.
- (12) Petrich, J.; Poyart, C.; Martin, J. *Biochemistry* **1988**, *27*, 4049.
- (13) Scott, T. W.; Friedman, J. M. *J. Am. Chem. Soc.* **1984**, *106*, 5677.
- (14) Turner, J.; Voss, D. F.; Paddock, C.; Miles, R. B.; Spiro, T. G. *J. Phys. Chem.* **1982**, *86*, 859.
- (15) Kitagawa, T.; Nagai, K.; Tsubaki, M. *FEBS Lett.* **1979**, *104*, 376.
- (16) Hu, S.; Smith, K. M.; Spiro, T. G. *J. Am. Chem. Soc.* **1996**, *118*, 12638.
- (17) Mizutani, Y.; Nagai, M. *Chem. Phys.*, in press.
- (18) Mizutani, Y.; Kitagawa, T. *J. Phys. Chem. B* **2001**, *105*, 10992.
- (19) Hofrichter, J.; Sommer, J. H.; Henry, E. R.; Eaton, W. A. *Proc. Natl. Acad. Sci. U.S.A.* **1983**, *80*, 2235.
- (20) Balakrishnan, G.; Case, M. A.; Pevsner, A.; Zhao, X.; Tengroth, C.; McLendon, G. L.; Spiro, T. G. *J. Mol. Biol.* **2004**, *340*, 843.
- (21) Jayaraman, V.; Rodgers, K.; Mukerji, I.; Spiro, T. *Science* **1995**, *269*, 1843.
- (22) Balakrishnan, G.; Tsai, C. H.; Wu, Q.; Case, M. A.; Pevsner, A.; McLendon, G. L.; Ho, C.; Spiro, T. G. *J. Mol. Biol.* **2004**, *340*, 857.
- (23) Campbell, B.; Chance, M.; Friedman, J. *Science* **1987**, *238*, 373.
- (24) Huang, J.; Ridsdale, A.; Wang, J.; Friedman, J. M. *Biochemistry* **1997**, *36*, 14353.
- (25) Chavez, M. D.; Courtney, S. H.; Chance, M. R.; Kiula, D.; Nocek, J.; Hoffman, B. M.; Friedman, J. M.; Ondrias, M. R. *Biochemistry* **1990**, *29*, 4844.
- (26) Ahmed, A. M.; Campbell, B. F.; Caruso, D.; Chance, M. R.; Chavez, M. D.; Courtney, S. H.; Friedman, J. M.; Iben, I. E. T.; Ondrias, M. R.; Yang, M. *Chem. Phys.* **1991**, *158*, 329.
- (27) Chance, M. R.; Courtney, S. H.; Chavez, M. D.; Ondrias, M. R.; Friedman, J. M. *Biochemistry* **1990**, *29*, 5537.